THE JOURNAL OF BIOLOGICAL CHEMISTRY VOL. 287, NO. 3, pp. 2144–2155, January 13, 2012

Interferon-γ Alters Downstream Signaling Originating from Epidermal Growth Factor Receptor in Intestinal Epithelial Cells

*FUNCTIONAL CONSEQUENCES FOR ION TRANSPORT**

Received for publication, October 28, 2011 Published, JBC Papers in Press, November 8, 2011, DOI 10.1074/jbc.M111.318139

Gisela Paul, Ronald R. Marchelletta, Declan F. McCole, and Kim E. Barrett[1]

From the Division of Gastroenterology, University of California, San Diego, School of Medicine, La Jolla, California 92093

Background: Inflammation alters epithelial signaling. We studied how IFN-γ regulates EGFr signaling.
Results: IFN-γ regulated EGFr expression, membrane localization, tyrosine residue phosphorylation, and linkage to MAPK. EGF no longer inhibited ion transport in IFN-γ-treated cells.
Conclusion: EGFr signaling outcomes are altered by inflammation.
Significance: These effects may contribute to diarrheal and other symptoms of inflammatory bowel diseases.

The epidermal growth factor receptor (EGFr) regulates many cellular functions, such as proliferation, apoptosis, and ion transport. Our aim was to investigate whether long term treatment with interferon-γ (IFN-γ) modulates EGF activation of downstream signaling pathways in intestinal epithelial cells and if this contributes to dysregulation of epithelial ion transport in inflammation. Polarized monolayers of T_{84} and HT29/cl.19A colonocytes were preincubated with IFN-γ prior to stimulation with EGF. Basolateral potassium transport was studied in Ussing chambers. We also studied inflamed colonic mucosae from C57BL/6 mice treated with dextran sulfate sodium or *mdr1a* knock-out mice and controls. IFN-γ increased intestinal epithelial EGFr expression without increasing its phosphorylation. Conversely, IFN-γ caused a significant decrease in EGF-stimulated phosphorylation of specific EGFr tyrosine residues and activation of ERK but not Akt-1. In IFNγ-pretreated cells, the inhibitory effect of EGF on carbachol-stimulated K^+ channel activity was lost. In inflamed colonic tissues, EGFr expression was significantly increased, whereas ERK phosphorylation was reduced. Thus, although it up-regulates EGFr expression, IFN-γ causes defective EGFr activation in colonic epithelial cells via reduced phosphorylation of specific EGFr tyrosine residues. This probably accounts for altered downstream signaling consequences. These observations were corroborated in the setting of colitis. IFN-γ also abrogates the ability of EGF to inhibit carbachol-stimulated basolateral K^+ currents. Our data suggest that, in the setting of inflammation, the biological effect of EGF, including the inhibitory effect of EGF on Ca^{2+}-dependent ion transport, is altered, perhaps contributing to diarrheal and other symptoms *in vivo*.

The precise etiology of the two entities of chronic inflammatory bowel disease, Crohn disease and ulcerative colitis, remains unknown despite a vast body of research. In Crohn disease, there is a chronic T helper 1 (Th1)-driven immune response with overproduction of inflammatory cytokines, such as IFN-γ and interleukin (IL)-12 (1). Moreover, increased serum levels and mucosal production of IFN-γ in Crohn disease have also been demonstrated (2). In mice, the frequently used acute dextran sulfate sodium (DSS)[2] colitis model is mainly a Th1 cytokine-driven inflammation with up-regulation of IFN-γ, IL-12, IL-1, and TNF-α (3). A key role for IFN-γ in the pathogenesis of DSS colitis has been shown in both C57BL/6 and Balb/c mice (4). Indeed, IFN-$\gamma^{-/-}$ mice are resistant to DSS-induced colitis (5). In another model of spontaneous colitis, the *mdr1a*$^{-/-}$ mouse, IFN-γ mRNA and protein levels are elevated more than 50-fold in mice with established colitis compared with controls, and production of IFN-γ is also elevated in stimulated mesenteric lymph nodes (6, 7). Interestingly, the human *MDR* gene is located on chromosome 7, a susceptibility locus for inflammatory bowel diseases (8).

Proinflammatory cytokines, such as IFN-γ and TNF-α, can induce tight junction reorganization and/or epithelial damage that causes a leaky mucosal barrier (9, 10). In health, a polarized monolayer of columnar intestinal epithelial cells normally forms a tight barrier to the access of toxic agents to the mucosal immune system (11). However, IFN-γ disrupts tight junctions and thereby disturbs paracellular transport mechanisms. The barrier function of the epithelium is also vital to maintain the electrical gradients necessary for controlled regulation of absorption *versus* secretion of electrolytes and water. Dysregulation of the balance between absorption and secretion by the

* This work was supported, in whole or in part, by National Institutes of Health Training Grant T32 DK007202 (to R. R. M.). This work was also supported by an unrestricted grant from the Shape-Up settlement fund (to K. E. B.), the UCSD Digestive Diseases Research Development Center (National Institutes of Health Grant DK080506), a grant from the German Research Foundation (Deutsche Forschungsgemeinschaft) (to G. P.), and a Crohn's and Colitis Foundation of America Senior Research Award (to D. F. M.).

[1] To whom correspondence should be addressed: Division of Gastroenterology, Dept. of Medicine, University of California, San Diego, 9500 Gilman Dr.-0063, La Jolla, CA 92093-0063. Tel.: 858-534-6655; Fax: 858-534-3338; E-mail: kbarrett@ucsd.edu.

[2] The abbreviations used are: DSS, dextran sulfate sodium; EGFr, epidermal growth factor receptor; CCh, carbachol; I_{sc}, short circuit current.

epithelium can lead to secretory diarrhea, a major symptom of inflammatory bowel diseases.

The epidermal growth factor receptor (EGFr) has been shown to play a role in repair and cell growth, but it also exerts important influences on epithelial transport in the gastrointestinal tract. The most important downstream signaling cascades are the Ras-Raf-MEK-ERK as well as the phosphatidylinositol 3-kinase (PI3K)-AKT-mTOR pathways. Ligand binding leads to EGFr dimerization and autophosphorylation and to tyrosine phosphorylation of other proteins. The mitogen-activated protein kinase (MAPK) and PI3K pathways contribute to proliferation and play different roles in epithelial ion transport. We showed previously that transactivation of EGFr by G protein-coupled receptor agonists could limit excessive chloride secretion via the MAPK pathway (12). Another study documented the role of the PI3K pathway in calcium transport (13). EGF inhibits carbachol-induced ion transport in intestinal epithelial cells by a mechanism that involves activation of PI3K as well as MAPK pathways (14, 15). EGFr signaling also plays an important role in overall intestinal homeostasis. This is perhaps best demonstrated in studies using transgenic mice with defective EGFr (*waved-2*) or lacking the EGFr ligand, TGF-α (*waved-1*). Both models display an increased susceptibility to colitis induced by the administration of DSS (16, 17). Conversely, overexpression of TGF-α reduces susceptibility to DSS colitis (18). These data point to a predominant role for EGFr in protecting against the development of chronic intestinal disease.

Our group showed previously that ion transport responses are diminished in tissues from colitic mice and that EGF could restore normal ion transport responses to calcium- and cyclic nucleotide-dependent agonists (19). Thus, despite its inhibitory effect in normal tissue, EGF normalized ion transport in the setting of inflammation by a mechanism that involved ERK-MAPK and PI3K. However, the reason for the differential effect of EGF in normal and inflamed tissues was unknown. Nevertheless, these observations have clinical relevance because EGF enemas have been shown to be beneficial in reducing diarrhea and other symptoms in patients with left sided ulcerative colitis (20). We hypothesized that factors in inflamed tissues might modulate the precise consequences of EGFr activation in the intestinal epithelium. Taking IFN-γ as an exemplar of an inflammatory mediator relevant to colitis, this study was designed to test this hypothesis *in vitro* and *in vivo*.

EXPERIMENTAL PROCEDURES

Materials—Human recombinant IFN-γ (Roche Applied Science), carbachol (Sigma), epidermal growth factor (Millipore, Temecula, CA), amphotericin B (Calbiochem), rabbit anti-lamin A/C-antibody, rabbit anti-ERK1-antibody (Santa Cruz Biotechnology, Inc., Santa Cruz, CA), rabbit anti-phospho-Akt(Ser^{473}) antibody, rabbit anti-phospho-ERK1/2 antibody that detects the 42- and 44-kDa isoforms, rabbit anti-phospho-EGFr(Tyr^{1173}) antibody, rabbit anti-EGFr antibody (Cell Signaling Technology, Danvers, MA), rabbit anti-Akt antibody (Upstate Biotechnology, Inc., Lake Placid, NY), anti-EGFr neutralizing antibody, clone LA 1 (Millipore), and horseradish peroxidase (HRP) mouse anti-phosphotyrosine (BD Transduction Laboratories) were obtained from the sources indicated. Antibodies to phospho-EGFr(Tyr^{992}) phospho-EGFr(Tyr^{1068}), phospho-EGFr(Tyr^{1086}), and phospho-EGFr(Tyr^{1148}) were obtained from BIOSOURCE (Camarillo, CA). All other reagents were of at least analytical grade and acquired commercially.

Physiological Solutions—The composition of the Ringer's solution used for Western blot studies was as follows: 140 mM Na^+, 120 mM Cl^-, 5.2 mM K^+, 25 mM HCO_3^-, 0.4 mM $H_2PO_4^-$, 2.4 mM HPO_4^{2-}, 1.2 mM Ca^{2+}, 1.2 mM Mg^{2+}, and 10 mM D-glucose. For Ussing chamber experiments, the salt solution for the apical side was modified to 78.4 mM NMDG, 25 mM Na^+, 120 mM Cl^-, 41.6 mM K^+, 25 mM HCO_3^-, 0.4 mM $H_2PO_4^-$, 2.4 mM HPO_4^{2-}, 1.2 mM Ca^{2+}, 1.2 mM Mg^{2+}, and 10 mM D-glucose and for the basolateral side to 114.8 mM *N*-methyl-D-glucamine, 25 mM Na^+, 120 mM Cl^-, 5.2 mM K^+, 25 mM HCO_3^-, 0.4 mM $H_2PO_4^-$, 2.4 mM HPO_4^{2-}, 1.2 mM Ca^{2+}, 1.2 mM Mg^{2+}, and 10 mM D-glucose.

Tissue Culture—Human T_{84} colonic epithelial cells were cultured as described previously (21). In brief, cells (passages 20–40) were grown in 1:1 Dulbecco's modified Eagle's/Ham's F-12 medium with L-glutamine and 15 mM HEPES (Mediatech Inc., Manassas, VA), supplemented with 5% newborn calf serum (Invitrogen) at 37 °C in 5% CO_2. Cells were fed twice a week and then seeded onto 30-mm Millicell transwell polycarbonate filters (10^6 cells) for Western blot analysis or 12-mm filters (5×10^5 cells) for Ussing chamber experiments. Cells were cultured for 10–15 days on filters prior to use. When grown on polycarbonate filters (Millipore), T_{84} cells acquire the polarized phenotype of native colonic epithelia.

HT-29/cl.19A cells (22) were grown to confluence in McCoys's 5A medium with L-glutamine, supplemented with 10% fetal bovine serum (FBS) (HyClone Laboratories Inc., Logan, Utah) at 37 °C in 5% CO_2 (passages 20–40). Cells were fed three times a week and passaged once a week in 75-cm^2 flasks and then seeded onto 30-mm Millicell transwell polycarbonate filters (10^6 cells) for Western blot analysis.

Cells grown on polycarbonate filters were stimulated basolaterally with IFN-γ (1000 units/ml) for up to 72 h. After preincubation with IFN-γ, cells were stimulated with EGF (100 ng/ml) from the basolateral side for up to 90 min.

Immunoprecipitation and Western Blot Analysis—T_{84} monolayers were preincubated with IFN-γ or medium for the indicated time periods and then washed three times with warm Ringer's solution and allowed to equilibrate at 37 °C for 30 min. Afterward, cell monolayers were stimulated with EGF (100 ng/ml) for up to 90 min. The reaction was stopped by washing with ice-cold Ringer's solution. This was followed by lysing the cells in lysis buffer (1% Triton X-100, 1 μg/ml leupeptin, 1 μg/ml pepstatin, 1 μg/ml antipain, 100 μg/ml phenylmethylsulfonyl fluoride, 1 mM Na^+-vanadate, 1 mM sodium fluoride, and 1 mM EDTA in phosphate-buffered saline) for 45 min. Cells were scraped off the filters, and the protein content of the lysates was assayed using a Bio-Rad protein assay kit. Samples were adjusted for an equal amount of protein and incubated with 5 μg of monoclonal anti-EGFr antibody for 1 h at 4 °C on a rotating platform. This was followed by incubation with protein A-agarose beads (Upstate Chemicon, Temecula, CA) for 1 h at 4 °C on a rotating platform. The protein A-agarose-antibody-antigen complex was pelleted by centrifugation for 3 min at

1200 rpm and washed three times with ice-cold Ringer's solution. The beads were then resuspended in 2× gel-loading buffer (50 mM Tris, pH 6.8, 2% SDS, 200 mM dithiothreitol, 40% glycerol, 0.2 bromphenol blue) and boiled for 4 min before loading onto a 7.5% polyacrylamide gel to resolve proteins. For whole cell lysate immunoblotting, an aliquot of lysate was diluted in 2× gel-loading buffer (50 mM Tris, pH 6.8, 2% SDS, 200 mM dithiothreitol, 40% glycerol, 0.2 bromphenol blue) and boiled for 4 min before the samples were loaded on a 4–15% polyacrylamide gel to resolve proteins.

Resolved proteins were transferred onto polyvinylidene membranes (Millipore). The membrane was then blocked with 1 or 5% (for anti-phosphoantibodies) skim milk in Tris-buffered saline (TBS) for at least 30 min. This was followed by incubation with the primary antibody in 1% skim milk or 5% BSA (for anti-phospho-antibodies) overnight. After five washes with Tris-buffered saline containing 1 or 0.1% (for anti-phosphoantibodies) Tween, the membranes were incubated with an HRP-conjugated secondary antibody (1:3000) for 30 min. After additional washing with wash buffer, proteins were detected using an enhanced chemiluminescence detection kit (GE Healthcare). Densitometric analysis of Western blots was performed using NIH Image software.

Phospho-Akt1 ELISA—Whole cell lysates from T_{84} cells grown on filters were analyzed for phospho-Akt1 using a commercially available enzyme-linked immunsorbant assay (PathScan Phospho-Akt1(Ser^{473}) Sandwich ELISA kit, Cell Signaling Technology) according to the manufacturer's instructions.

RNA Isolation and Real-time PCR—RNA isolation from T_{84} cells was performed using the RNeasy Plus minikit (Qiagen, Valencia, CA) according to the manufacturer's instructions. DNA was removed using the TURBO DNA-free kit (Ambion, Austin, TX) according to the manufacturer's recommendations. RNA concentration was determined by absorbance at 260 and 280 nm. cDNA was synthesized using a high capacity cDNA reverse transcription kit (Applied Biosystems, Foster City, CA). Real-time PCR was performed using MESA GREEN qPCR MasterMix Plus for SYBR assays (Eurogentec, San Diego, CA) on a StepOnePlus real-time PCR system using Step One software, version 2.0 (Applied Biosystems, Foster City, CA). The conditions for real-time PCR were as follows: 5 min at 95 °C for enzyme activation followed by 40 cycles of 15 s of 95 °C for denaturation and 1 min of 60 °C for annealing and extension. The melt curve was performed at 50 °C for 1 h. Human GAPDH was used as an endogenous control (sense, CATGTTCGTCATGGGTGTGAACCA; antisense, AGTGATGGCATGGACTGTGGTCAT). The primer sequences for human EGFr were as follows: sense, TTTGCCAAGGCACGACTAACAAG; antisense, ATTCCCAAGGACCACCTCACAGTT. All measurements were made in triplicate, and results were analyzed by the $\Delta\Delta CT$ method.

Confocal Microscopy—5×10^5 T_{84} cells were seeded onto 12-mm Millicell-HA filters for 6–8 days before stimulation with IFN-γ. 48 h after stimulation, cells were fixed with 10% formalin in PBS for 10 min and permeabilized in 0.3% Triton X-100 in PBS for 10 min. Between steps, cells were washed three times with PBS. Blocking was performed with 20% donkey serum in PBS for 1 h, followed by a single washing step. As a primary antibody, rabbit anti-EGFr antibody was diluted in 2% BSA. Cells were incubated with primary antibody overnight at 4 °C in a humidified chamber. After washing (three times), secondary Alexa-488-conjugated donkey anti-rabbit antibody (excitation/emission maxima at 495/519 nm; Molecular Probes, Eugene, OR) was added at a 1:500 dilution in 20 mg/ml BSA in PBS for 30 min at room temperature. After washing (three times with PBS), cells were incubated with Hoechst 33258 (excitation/emission maxima at 352/461 nm; Molecular Probes) in PBS (1:500) for 20 min at room temperature. The final washing stage consisted of four washes with PBS. Then the cells on the filter membrane were transferred onto glass slides and mounted in ProLong Gold Antifade Reagent (Molecular Probes). Confocal microscopy was performed using a Zeiss LSM 510 laser-scanning confocal system on a Zeiss Axioscope 2 upright microscope (Zeiss, Jena, Germany). Analyses of data were performed using the Zeiss LSM 5 Image Examiner software (Zeiss).

Electrophysiological Studies—T_{84} cells seeded on permeable 12-mm Transwells were grown until confluence. Prior to Ussing chamber experiments, monolayers were pretreated with IFN-γ (1000 units/ml) for 24 h. The duration of pretreatment was chosen to avoid effects on transepithelial resistance that occur with longer exposure to the cytokine. The concentration was chosen based on previous ion transport studies with IFN-γ from our group (23). Cells were mounted in Ussing chambers (window area = 0.6 cm^2) and bathed in oxygenated (95% O_2 and 5% CO_2) Ringer's solution (basolateral salt solution) at 37 °C. After equilibration, monolayers were voltage-clamped to zero potential difference by application of short circuit current (I_{sc}). Amphotericin B (100 μM) was then added to the apical side of the chamber to permeabilize the apical membrane, and after 30 min, an apical-to-basolateral K^+ gradient (40 mM to 5 mM) was established. Ouabain (100 μM) was added basolaterally to inhibit Na^+-K^+-ATPase. Because of the applied potassium gradient, changes in I_{sc} (ΔI_{sc}) are wholly reflective of electrogenic potassium currents through the basolateral membrane. Changes in I_{sc} were recorded in response to carbachol (100 μM) with or without prior stimulation with EGF (100 ng/ml) for 20 min.

Animals—8-Week-old C57BL/6 mice, 15-week-old FVB, and 12-week-old *mdr1a*$^{-/-}$ (on an FVB background) mice were housed under conventional conditions and provided with food and water *ad libitum*. Animal studies were approved by the University of California, San Diego, Committee on Investigations Involving Animal Subjects.

Induction of Colitis—Acute colitis was induced in C57BL/6 mice by giving 3% DSS (molecular weight 36,000–56,000, MP Biomedicals, LLC, Solon, OH) orally in drinking water for 7 days as first described by Okayasu *et al.* (24). Mice were sacrificed on day 8 after 7 days of DSS treatment or water as control. FVB mice were killed at 12 weeks of age; *mdr1a*$^{-/-}$ mice were observed for signs of spontaneously developing colitis, such as diarrhea, blood in stool, and ruffled fur, and sacrificed after such signs developed, typically at 12–15 weeks of age. All mice were sacrificed by cervical dislocation. Colons were removed, and the mucosal layer was stripped of serosal layers. Mucosal tissues were transferred in ice-cold Ringer's solution, dissected with clean tools, and incubated in ice-cold lysis buffer. Protein lysis and Western blot analysis were performed as described for cell culture experiments.

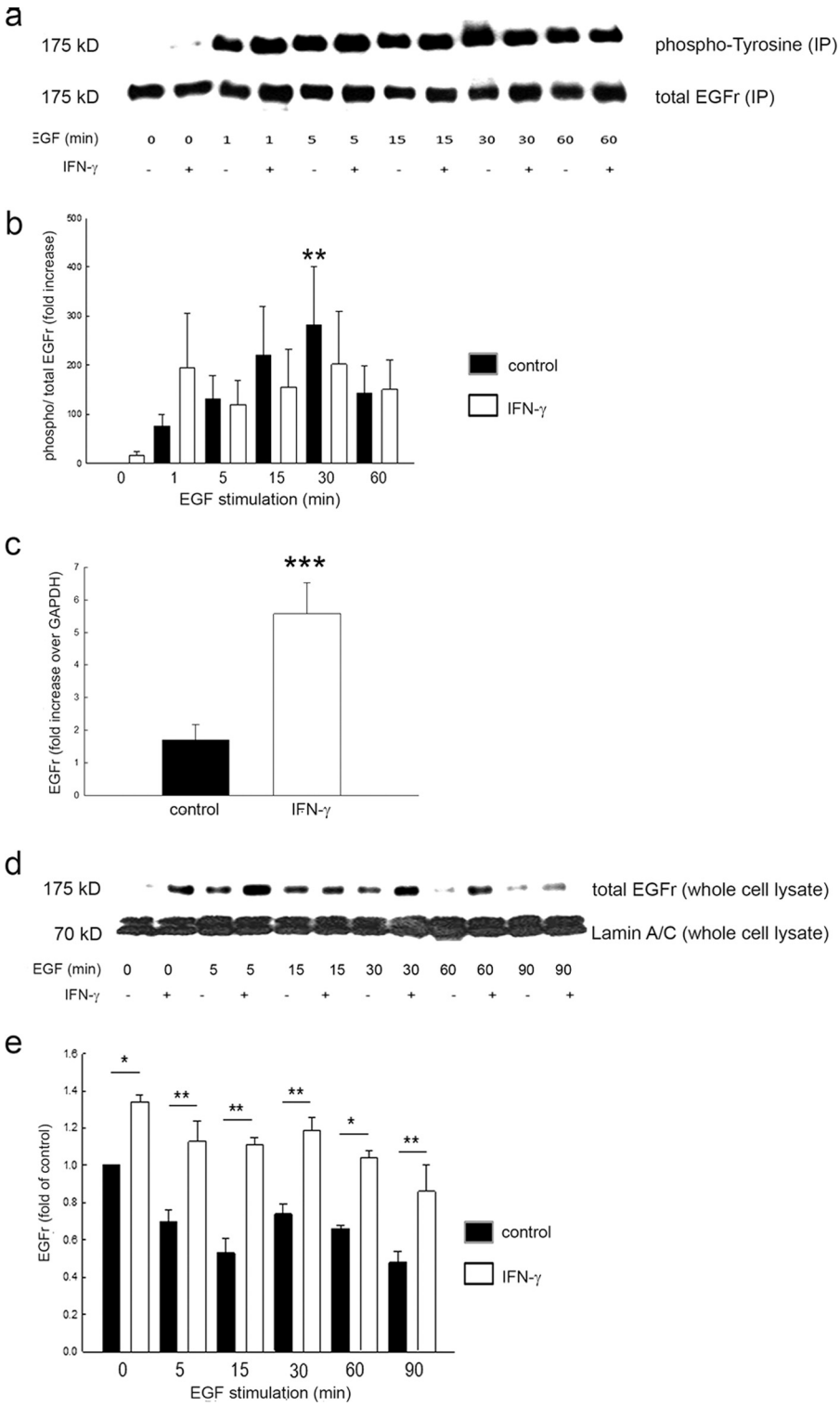

FIGURE 1. **IFN-γ pretreatment does not alter EGF-induced EGFr phosphorylation but increases EGFr expression at both mRNA and protein level in T_{84} cells.** *a*, EGFr was immunoprecipitated, and phosphotyrosine or total EGFr was sequentially blotted in immunoprecipitates from T_{84} cells in response to EGF stimulation at the indicated time points. Cells were pretreated for 48 h with IFN-γ or medium. A representative Western blot is shown. *b*, densitometric analysis ($n = 8$) showed a significant increase of phosphorylated EGFr in controls at 15 min of EGF stimulation. IFN-γ did not affect EGF-induced EGFr phosphorylation in T_{84} cells. Data are expressed as percentage of control without EGF stimulation. *Asterisks* denote significant differences from control (*, $p \leq 0.05$). *c*, EGFr mRNA expression in response to IFN-γ treatment over 48 h, normalized to GAPDH ($n = 6$, performed in triplicate). *d*, representative Western blot of whole cell lysates, sequentially probed for total EGFr or lamin A/C as loading control. *e*, densitometric analysis reveals significantly increased EGFr expression in IFN-γ-treated cells at the indicated time points with EGF stimulation. Data are expressed as -fold control. *Asterisks* denote significant differences from control (*, $p \leq 0.05$; **, $p \leq 0.01$). *Error bars*, S.E.

Statistical Analysis—All data are expressed as means ± S.E. for a series of *n* experiments. Student's *t* test or analysis of variance with Student-Newman-Keuls post-test was used to compare mean values as appropriate using GraphPad Instat 3 software (Graph Pad Software, La Jolla, CA). Values of $p < 0.05$ were considered significant.

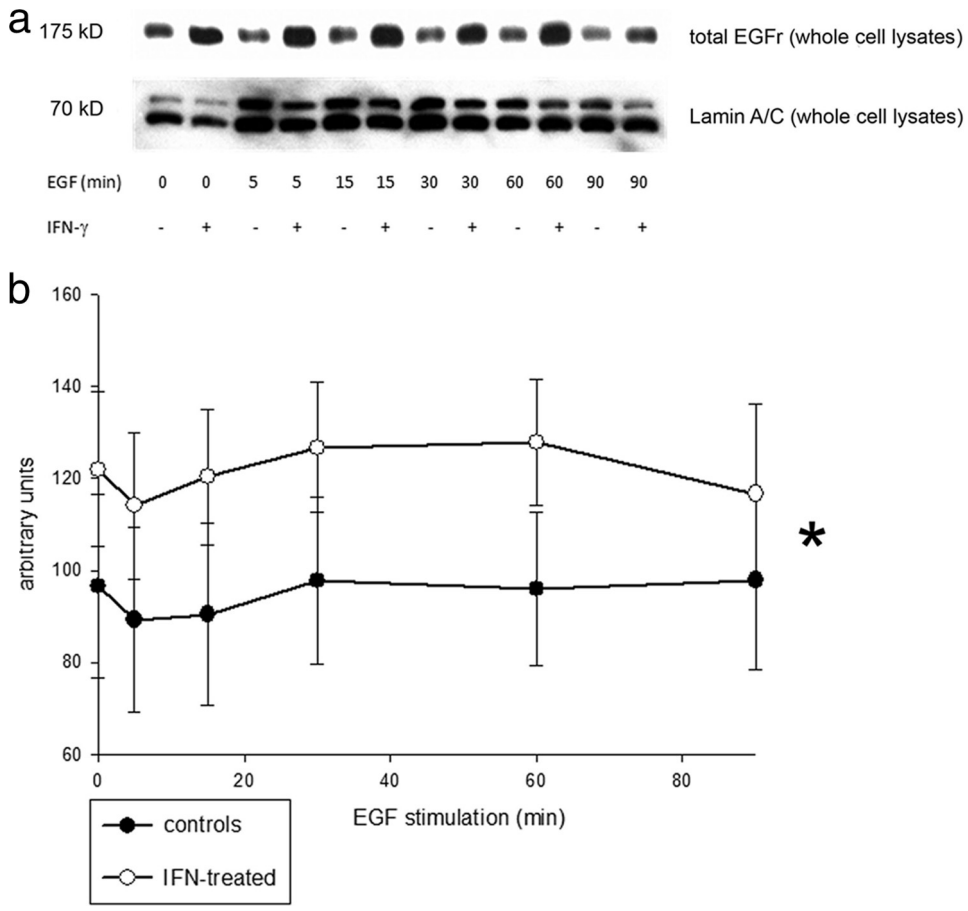

FIGURE 2. **IFN-γ increases EGFr expression in HT29/cl.19A cells.** *a*, representative Western blot of whole cell lysates of HT29/cl.19A cells, sequentially probed for total EGFr or lamin A/C as loading control. *b*, densitometric analysis shows significantly increased EGFr levels in IFN-γ-treated compared with control cells. Data are expressed in arbitrary units. *Asterisks* denote a significant difference between groups (*, $p \leq 0.05$, two-way analysis of variance). *Error bars*, S.E.

RESULTS

IFN-γ Does Not Alter Overall EGF-induced EGFr Phosphorylation—It has been shown that IFN-γ alone is capable of transactivating the EGFr in T_{84} cells (23, 25). Based on these observations, we sought to determine if preincubation of T_{84} cells with IFN-γ alters EGF-induced phosphorylation of its receptor. We treated T_{84} cells with IFN-γ (1000 units/ml) for 48 h prior to EGF stimulation (100 ng/ml) for up to 60 min. As expected, EGF significantly increased EGFr phosphorylation over time in control cells (Fig. 1, *a* and *b*). However, whereas basal EGFr phosphorylation was increased by IFN-γ, the cytokine did not alter EGF-induced phosphorylation of its receptor.

IFN-γ Increases Epithelial EGFr Expression—We hypothesized that the apparent inability of IFN-γ to modulate EGF-induced phosphorylation of its receptor might be due to changes in expression of the receptor after IFN-γ treatment. To investigate this, we first performed real-time PCR on T_{84} cell lysates pretreated for 48 h with IFN-γ. We found significantly higher expression of EGFr mRNA in treated compared with control cells (Fig. 1*c*). We next investigated whether this was accompanied by increased expression of the receptor at the protein level. As shown in Fig. 1, *d* and *e*, treatment with IFN-γ for 48 h, followed by stimulation with EGF for 0–90 min, revealed significantly higher levels of EGFr after pretreatment with IFN-γ compared with controls ($p < 0.05$ *versus* control, $n = 3$). This increase was sustained at each time point of EGF stimulation. To confirm that this phenomenon was not limited to T_{84} cells, we also treated HT29/cl.19A cells with IFN-γ prior to challenging the cells with EGF for up to 90 min. IFN-γ also increased EGFr expression in this cell line (Fig. 2, *a* and *b*).

IFN-γ Causes Relocalization of EGFr in T_{84} Cells—To verify the effect of IFN-γ (1000 units/ml, 72 h) on EGFr levels, we analyzed EGFr expression by confocal imaging (Fig. 3). As predicted, IFN-γ markedly increased staining for EGFr (*green*). However, whereas EGFr in control cells appeared to localize distinctly to the membrane, as demonstrated by close apposition to the submembrane actin (*red*), the receptor relocalized, in part, to the cytoplasm in cells treated with IFN-γ and showed a more diffuse staining pattern (Fig. 3*a*). After 72 h of IFN-γ exposure, a certain disruption of the cytoskeleton is evident. This might be mediated by AMP-activated protein kinase, as shown previously by our group (26). In the current study, we concentrated on the change in localization of the receptor. This change was reflected by a diminished intensity of EGFr co-localized with submembrane actin in IFN-γ-treated cells. Changes in EGFr localization were verified by scans along randomly assigned lines on representative confocal images in Fig. 3*a* using the LSM 510 colocalization software to con-

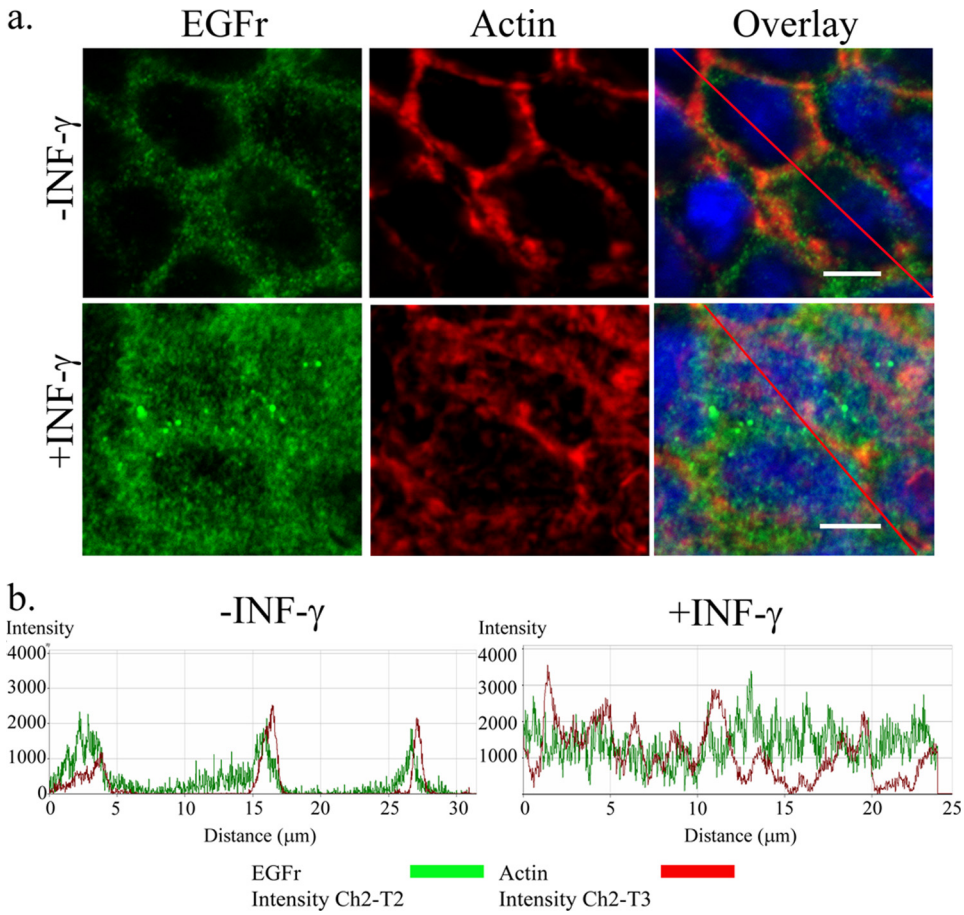

FIGURE 3. **IFN-γ pretreatment changes cellular distribution of EGFr.** *a*, in control cells (*top*), EGFr (*green*) is colocalized to the actin cytoskeleton (*red*) with only sparse localization to the cytoplasm and nucleus. In IFN-γ (1000 units/ml, 72 h)-treated cells (*bottom*), EGFr redistributes to the cytosol, resulting in partial loss of colocalization with submembrane actin. In addition, treatment with IFN-γ increases overall EGFr expression as followed by confocal microscopy ($n = 3$, 3–5 visual fields, *white bar* = 10 μm). *b*, an analysis along the randomly assigned lines in *a* was done on the representative overlay images of both control and IFN-γ-treated cells in Fig. 4*a* (*red line*). A shift in coincident peaks of EGFr (*green line*) from actin (*red line*) was observed in cells treated with IFN-γ compared with control cells.

firm overlap of fluorescence intensities (arbitrary units) (Fig. 3*b*). The peaks associated with each marker (EGFr (*green*) and submembrane actin (*red*)) showed diminished overlap in cells treated with IFN-γ *versus* untreated cells. This shift of EGFr enrichment was further substantiated by quantification of total actin pixels (*red*) colocalized with total EGFr pixels (*green*). The extent of total actin red pixels that were colocalized with total EGFr green pixels in untreated cells was 19.5 ± 1.0%. This value decreased by one-third in IFN-γ-treated cells (13.0 ± 2.1%) ($p < 0.05$, $n = 3$, 3–5 visual fields). Thus, the failure of IFN-γ to potentiate EGF-induced EGFr phosphorylation, despite increasing levels of the receptor, may reflect the fact that the cytokine relocalizes the receptor to a site where it may be resistant to ligand binding and/or activation.

IFN-γ Treatment Selectively Abrogates Phosphorylation of Different EGFr Tyrosine Residues—The signaling consequences of EGFr activation depend on the precise census of receptor tyrosine residues that are phosphorylated. Thus, it was of interest to assess whether IFN-γ also altered this pattern of tyrosine phosphorylation. We assessed phosphorylation of five EGFr tyrosine residues that are known to be autophosphorylation substrates (Tyr^{992}, Tyr^{1068}, Tyr^{1086}, Tyr^{1148}, and Tyr^{1173}; Fig. 4, *a*–*e*). Pretreatment with IFN-γ significantly decreased the ability of EGF to induce phosphorylation of Tyr^{1068} and Tyr^{1086} (Fig. 4, *a* and *b*). On the other hand, phosphorylation of Tyr^{992} was delayed but ultimately not reduced in IFN-γ-treated cells (Fig. 4*c*), whereas that of Tyr^{1148} and Tyr^{1173} was not significantly affected (Fig. 4, *d* and *e*).

IFN-γ Modifies ERK but Not PI3K Activation—To explore further the downstream signaling outcomes originating at EGFr in IFN-γ-treated cells, we assessed activation of two major signaling pathways involved in EGFr regulation of ion transport, the ERK MAPK and PI3K pathways. In IFN-γ-treated cells, we detected a significant increase in ERK phosphorylation at baseline and following EGF stimulation compared with controls (Fig. 5, *a* and *b*). However, when compared with base-line levels in cells not exposed to EGF, the relative ability of EGF to increase ERK phosphorylation was actually reduced by IFN-γ treatment (Fig. 5*c*). Therefore, EGF had a diminished incremental effect on ERK activation when this pathway had previously been activated by IFN-γ. In contrast, when we investigated the effect of IFN-γ on EGF-stimulated PI3K signaling, as measured by phosphorylation of the downstream target, Akt-1, neither base-line nor EGF-stimulated

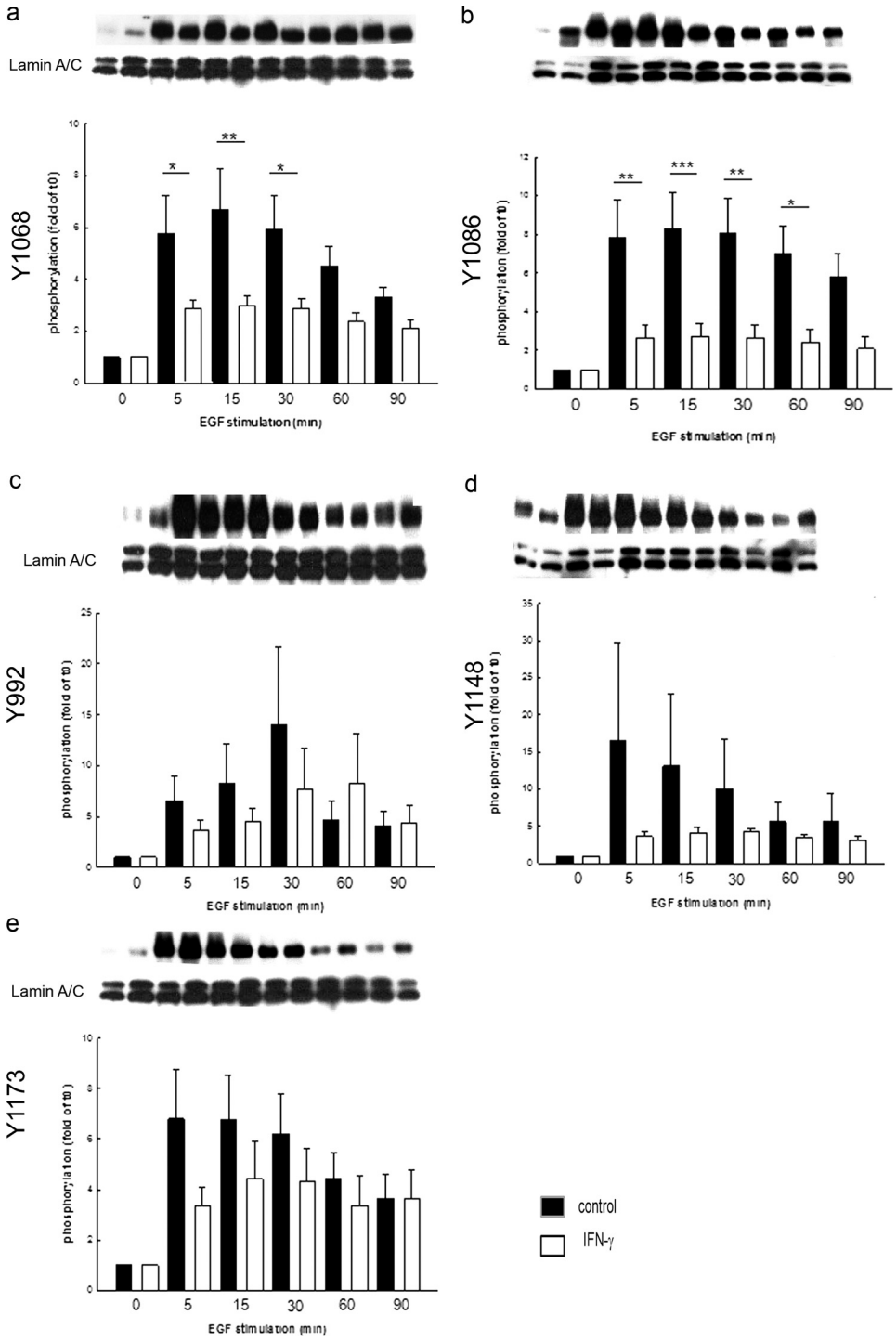

FIGURE 4. **IFN-γ decreases phosphorylation of select EGFr tyrosine residues.** Cells were treated for 48 h with IFN-γ or control, and phosphorylation of five key tyrosine residues was analyzed by Western blot. Densitometric analysis revealed a significant decrease in phosphorylation of EGFr residues Tyr^{1068} and Tyr^{1086} at 15 min after EGF stimulation (*a* and *b*; **, $p \leq 0.01$ ($n = 7$); ***, $p \leq 0.001$ ($n = 8$)) in cells treated with IFN-γ. Phosphorylation of Tyr^{992} was delayed in IFN-γ-treated cells (*c*, $n = 14$, not significant), whereas that of Tyr^{1148} and Tyr^{1173} was reduced slightly but not significantly (*d* and *e*, $n = 15$ and $n = 5$, not significant). *Error bars*, S.E.

phosphorylation of Akt was significantly influenced by pretreatment with IFN-γ (Fig. 5, *d* and *f*). The findings were confirmed when PI3K activation was alternatively assessed using an ELISA for phosphorylated Akt-1 (Fig. 5*f*). Overall, we conclude that IFN-γ emphasized the relative ability of EGFr to signal via PI3K at the expense of ERK.

Experimental Colitis Induces Opposing Effects on EGFr Expression and ERK Activation—To explore whether our cell culture results could be translated into the setting of disease, we investigated EGFr and its downstream signaling targets, ERK and Akt-1, in two murine models of experimental colitis: acute colitis induced by DSS and spontaneous colitis in *mdr1a*$^{-/-}$

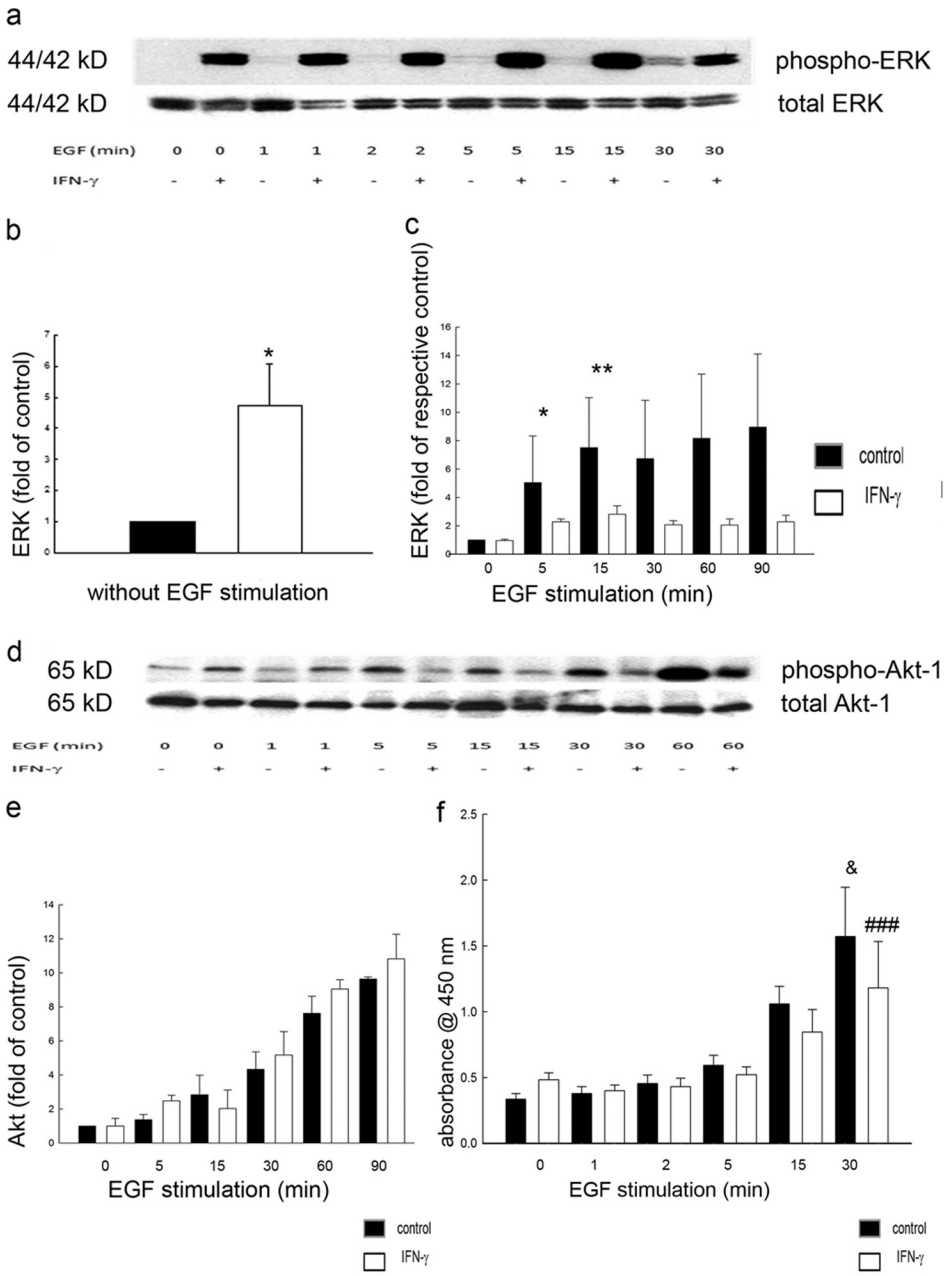

FIGURE 5. **IFN-γ increases ERK activation and reduces the capacity of EGF to activate ERK but not Akt-1.** *a*, representative Western blot of whole cell lysates of T_{84} cells, probed for phosphorylated or total ERK. *b*, in IFN-γ-treated cells, densitometric analysis revealed a significant increase in ERK phosphorylation at baseline (IFN-γ *versus* control; *, $p \leq 0.05$; $n = 8$). *c*, following EGF stimulation, increased ERK phosphorylation was detected in both groups. However, the relative increase in phosphorylation compared with time 0 revealed a reduced capacity of EGF to induce ERK activation in IFN-γ-treated cells. *d*, representative Western blot of whole cell lysates of T_{84} cells, probed for phosphorylated (Ser^{473}) or total Akt-1. *e*, the relative increase in phosphorylation over time with EGF stimulation showed no influence of prior IFN-γ treatment on EGF-induced Akt phosphorylation. *f*, phosphorylation of Akt-1, measured by ELISA, was significantly increased by EGF over time, but this was not influenced by the presence or absence of IFN-γ treatment (*, $p \leq 0.05$ after 30 min of EGF stimulation; $n = 3$ in duplicate). Error bars, S.E.

mice. For both models of experimental colitis, it has been shown that levels of IFN-γ are elevated (6, 7). Colonic tissues from C57BL/6 mice subjected to acute DSS colitis showed a significant increase in EGFr expression compared with tissues from control C57/BL6 mice (Fig. 6, *a* and *b*). Similarly, in *mdr1a*$^{-/-}$ mice that had developed spontaneous colitis, colonic tissues also showed significantly greater EGFr protein levels than seen in their FVB littermates (data not shown). This is in line with the results in T_{84} cells treated with IFN-γ, showing increased levels of the receptor. Next, we sought to investigate if the downstream signaling targets of EGFr are modulated in inflamed colonic tissue from mice.

In DSS colitis, mucosal tissues exhibited similar levels of total ERK as seen in normal mice, but ERK phosphorylation was essentially absent (Fig. 6, *c* and *d*). Moreover, total Akt-1 expression was similar and Akt-1 phosphorylation was not significantly changed compared with controls (data not shown). Similar trends were observed in *mdr1a*$^{-/-}$ mice (data not shown). Therefore, although we cannot necessarily ascribe our findings specifically to an action of IFN-γ, we conclude that

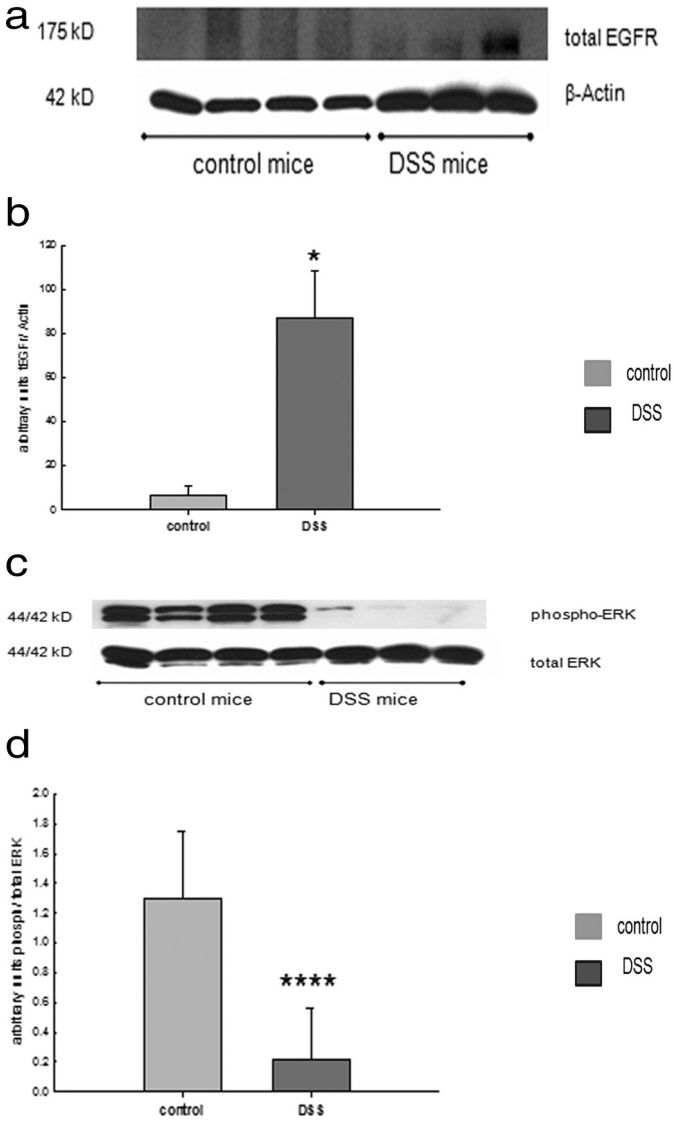

FIGURE 6. **In experimental colitis, mucosal EGFr expression is increased, whereas ERK phosphorylation is reduced.** 8-Week-old C57BL/6 mice were treated with 3% DSS in drinking water to induce an acute colitis or tap water as control. *a*, representative Western blot of lysates from mucosal tissue from distal colon, probed for total EGFr or β-actin as a loading control. *b*, elevated EGFr expression in mice treated with DSS for 7 days in drinking water (*, $p < 0.05$). *c*, representative Western blot of lysates from mucosal tissue from distal colon, probed for phosphorylated or total ERK. *d*, reduced ERK expression in mice treated with DSS (****, $p < 0.0001$). *Error bars*, S.E.

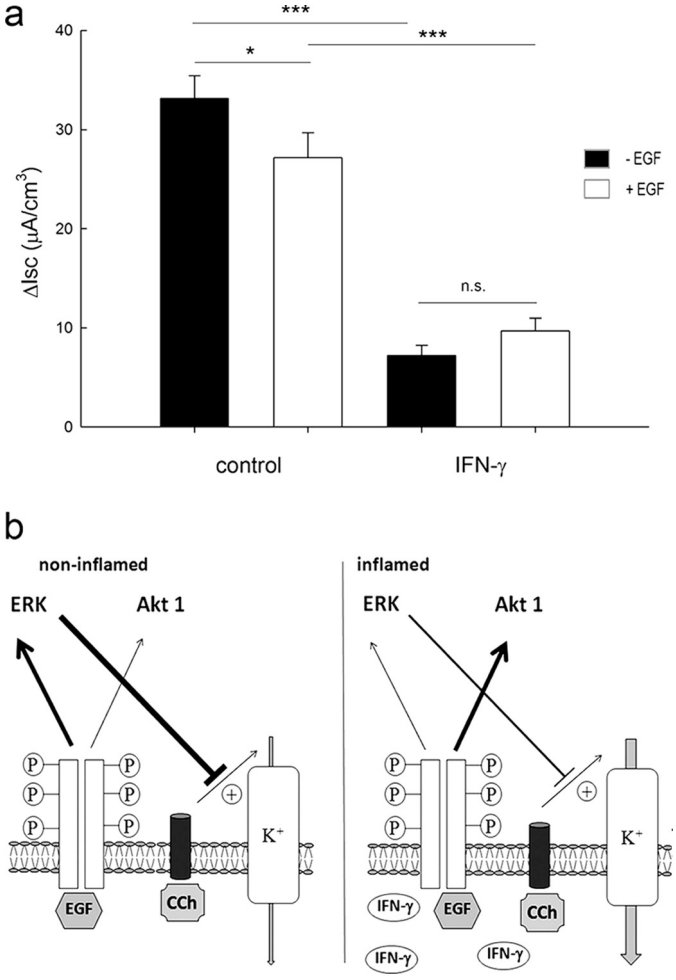

FIGURE 7. **IFN-γ leads to loss of the inhibitory effect of EGF on basolateral K^+ channel activity in T_{84} cells.** T_{84} cell monolayers were pretreated with or without IFN-γ for 24 h before mounting in Ussing chambers. Short circuit current (I_{sc}) measurements, reflective of basolateral K^+ channel activity, were recorded after stimulation with CCh in the presence or absence of EGF. *a*, in control cells, EGF significantly inhibited CCh-stimulated K^+ channel activity ($p < 0.05$, $n = 7$). However, in IFN-γ pretreated cells, which showed a reduced CCh-stimulated I_{sc}, the inhibitory effect of EGF was lost ($n = 7$, not significant (*n.s.*)). *b*, hypothetical model for the results of this study. In the non-inflamed state (*left half*), EGF binds to its receptor and activates both MAPK and PI3K pathways, which lead to an inhibitory effect on basolateral CCh-induced potassium currents. In contrast, during inflammation (*right half*), IFN-γ levels are elevated locally. This leads to a shift of the downstream signaling pathways in favor of EGF-stimulated PI3K. Furthermore, the inhibitory effect of ERK on basolateral CCh-induced potassium currents is lost. *Error bars*, S.E.

murine colitis is associated with an increase in EGFr expression and a biasing of downstream signaling targets away from ERK, as seen in cell culture.

IFN-γ Modifies Ability of EGF to Reduce Basolateral Potassium Currents in T_{84} Cells—Because IFN-γ pretreatment altered intracellular signaling pathways downstream of EGFr in intestinal epithelial cells, it was of interest to examine whether this also had functional consequences. We decided to investigate specifically the basolateral potassium current because EGF had previously been shown to inhibit this conductance in cells treated with calcium-dependent agonists, such as carbachol (CCh) (27–30). Confluent monolayers of T_{84} cells were treated with IFN-γ (24 h) and then mounted in Ussing chambers and studied under conditions where differences in I_{sc} are the result of potassium currents across the basolateral membrane (31). A 24-h period of IFN-γ preincubation was chosen to avoid the changes in barrier function that occur after 48–72 h of IFN-γ exposure and are probably mediated by AMP-activated protein kinase (26). As expected, IFN-γ reduced the basal level of potassium conductance (Fig. 7*a*). Moreover, EGF inhibited the CCh-stimulated ΔI_{sc} in control cells, as expected, but this effect was lost in cells that had been treated with IFN-γ (Fig. 7*a*). These findings imply that functional consequences of EGF treatment may be altered in epithelial cells exposed to IFN-γ.

DISCUSSION

In this study, IFN-γ was shown to alter EGFr expression, as well as signaling pathways originating from the receptor, in

colonic epithelial cells. Modulation of signaling pathways downstream of EGFr by IFN-γ probably accounts for functional changes in ion transport responses in our cell model and may also explain previous observations we have made in mouse models of experimental colitis, where EGF could partially restore impaired sodium absorptive responses in disease (19). IFN-γ plays a pivotal role in experimental colitis as well as in human inflammatory bowel disease. We therefore used a prolonged IFN-γ pretreatment to mimic a chronic state of inflammation.

In the current studies, IFN-γ tended to increase base-line EGFr phosphorylation, consistent with our earlier results showing that IFN-γ transactivates EGFr (23) but had no effect on overall EGF-induced EGFr phosphorylation. IFN-γ reportedly had different effects on EGFr phosphorylation in two other cell lines tested. In A431 cells, IFN-γ caused rapid and reversible independent tyrosine phosphorylation of EGFr, whereas in HepG2 cells, the presence of EGF was necessary for IFN-γ to transactivate the receptor (25, 32). This suggests various activation patterns and effects of inflammatory cytokines in different contexts. Even so, our studies imply that the differential effects of EGF in normal and inflamed settings that we have previously reported (19) probably cannot simply be attributed to a global change in EGFr activation.

Although we did not detect overall changes in EGF-induced phosphorylation of EGFr under the conditions studied, we observed increased expression of the receptor at both the mRNA and protein level. This effect was reproduced in the HT-29cl19a human colonic epithelial cell line and is consistent with a report of increased EGFr in the human breast cancer cell line MDA 468 (33) after incubation with IFN-γ. We also detected a change in receptor localization measured by immunofluorescent staining. We conclude that long term stimulation with IFN-γ actually decreases receptor abundance on the cell surface, presumably by stimulating receptor internalization (34). This might partly account for the fact that IFN-γ did not increase EGFr activation upon subsequent EGF stimulation, despite up-regulation of receptor expression. Our group demonstrated previously that barrier disruption in cells exposed to IFN-γ for a prolonged time period was mediated by AMP-activated protein kinase (26). In the current studies, we did not examine tight junction proteins, but we detected a disruption of the actin cytoskeleton in the immunofluorescence studies. Whether AMP-activated protein kinase activation leads to internalization of EGFr was not tested here but deserves further study.

To seek an alternative explanation for the ability of inflammation to modify EGFr signaling, the degree of phosphorylation of specific EGFr tyrosine residues was studied. In fact, of the five tyrosine residues tested, we detected significantly lower phosphorylation of two residues, whereas the other residues were not significantly affected. We therefore suggest, based on these and other data from our group (35–38), that IFN-γ may activate protein-tyrosine phosphatases directed against specific EGFr residues. This would be concordant with our observations that, *in vitro*, IFN-γ increases the expression and activity of one of the protein-tyrosine phosphatases, namely PTPN2 (38). We could also demonstrate increased PTPN2 expression in intestinal biopsy specimens from patients with Crohn disease (38). Other inflammatory stimuli, such as reactive oxygen species, can influence protein-tyrosine phosphatase activity as well (39, 40). Moreover, differences in the phosphorylation pattern of tyrosine residues in EGFr can lead to distinct cellular outcomes in intestinal epithelial cells (37). Upon activation of EGFr, distinct downstream signaling pathways, such as ERK-MAPK, PI3K/Akt-1, or the JAK/STAT pathway, are activated. We did not directly test the functional effects of the specific EGFr tyrosine residues affected by IFN-γ, but the shift toward the PI3K pathway (see below) probably indicates a functional consequence of the observed dephosphorylation of a specific constellation of tyrosine residues.

We found a significant increase in ERK but not Akt phosphorylation at baseline after incubation with IFN-γ. Conversely, IFN-γ reduced the relative ability of EGF to activate ERK but did not alter its ability to activate Akt-1. This implies that the consequences of EGFr activation may be redirected in inflammation. Previously, our group has shown that ERK accounts for termination of CCh-induced chloride secretory responses (15, 41, 42). Conversely, EGF favors the PI3K pathway over the ERK-MAPK pathway in modulating colonic ion transport responses in colitic mice (19). Our data shown here are concordant with these previous studies. We also investigated mucosal protein levels of ERK and Akt, as well as EGFr, in two models of experimental colitis. EGFr levels were elevated in inflamed tissues in agreement with previous studies (43, 44). Because EGFr plays a pivotal role in mucosal restitution, the elevated EGFr levels could be explained as an adaptation to promote mucosal healing (45–48) and PI3K activation. This was also proposed in previous studies of experimental colitis in mice with EGFr dysfunction or EGFr ligand deficiency (16, 17). ErbB4, a EGFr family member, is also increased in tissues from mice with colitis as well as in biopsies from patients suffering from Crohn disease (49).

To further investigate the consequences for ion transport, we used T_{84} cells to demonstrate that IFN-γ abolishes the inhibitory effect of EGF on CCh-induced basolateral potassium currents. Treatment of polarized intestinal epithelial cells with IFN-γ leads to down-regulation of many transporters and ion pumps, such as basolateral potassium channels, the Na^+-K^+-$2Cl^-$ cotransporter, and Na^+-K^+-ATPase (50–52). However, an ability of IFN-γ to selectively modulate the effect of EGF on ion transport responses had not been tested. Because basolateral potassium efflux is a driving force for apical calcium-dependent chloride secretion (53), the finding that IFN-γ reverses the inhibitory effect of EGF on a Ca^{2+}-dependent potassium current could partly explain diarrheal symptoms in disorders such as chronic inflammatory bowel diseases. Ion transport is reduced overall if IFN-γ is present. In our experimental setting, IFN-γ produced significantly reduced basolateral potassium current, as expected. Nevertheless, small changes in K^+ current could influence additional chloride secretion in inflammation. EGF was no longer able to inhibit the basolateral potassium current following IFNγ treatment, implying a subtle change in mucosal transport homeostasis. Earlier studies from our group have shown that direct activation of EGFr by EGF leads to inhibition of basolateral potassium channel activity via activation of

the PI3K pathway rather than the ERK-MAPK pathway (27). On the other hand, if EGFr is transactivated by G protein-coupled receptors, shedding of TGF-α leads to activation of ERK, limiting chloride secretion by inhibiting apical chloride channels (12, 15, 54, 55). Further, McCole *et al.* (19) demonstrated that EGF also influences ENaC activity in colitis via PI3K. Our findings may also imply, therefore, that other effects of EGF may be altered in epithelial cells exposed to IFN-γ. Fig. 7*b* summarizes our hypothetical model whereby in the non-inflamed state (*left half*), ERK predominantly limits basolateral CCh-induced potassium currents when EGF activates its receptor. This inhibitory effect is apparently diminished during inflammation (*right half*) due to a shift to the PI3K pathway and loss of ERK signaling. It is likely that the basolateral potassium channel targeted in our study is the Ca^{2+}-activated KCNN4 channel (56, 57). However, this will require clarification in future studies.

In summary, in Crohn disease and ulcerative colitis, one of the most common and disabling symptoms is diarrhea. Diarrheal disorders are ultimately the result of decreased absorption and/or increased secretion of fluid and electrolytes (58). It has been shown that EGFr plays a protective role in inflammatory conditions and that ERK negatively regulates chloride secretion. In this work, we demonstrate that IFN-γ causes defective EGFr activation in intestinal epithelial cells, with a shift toward the PI3K pathway in inflammation. These alterations in downstream signaling pathways originating at EGFr lead to functional consequences for ion transport responses in disease. Preincubation of intestinal epithelial cells with IFN-γ reverses the inhibitory effect of EGF on carbachol-induced potassium currents, which are required for anion secretion. Insights into perturbed activation of growth factor receptors and their functional consequences may lead to novel treatment strategies for chronic inflammatory bowel disease. We must, however, be mindful of the caveat that administration of EGFr ligands by themselves should be approached with caution due to the increased risk of colorectal cancer in ulcerative colitis patients, although such an approach has already been demonstrated to have clinical merit for the treatment of left-sided ulcerative colitis (20).

REFERENCES

1. Bouma, G., and Strober, W. (2003) The immunological and genetic basis of inflammatory bowel disease. *Nat. Rev. Immunol.* **3,** 521–533
2. Sasaki, T., Hiwatashi, N., Yamazaki, H., Noguchi, M., and Toyota, T. (1992) The role of interferon γ in the pathogenesis of Crohn's disease. *Gastroenterol. Jpn.* **27,** 29–36
3. Egger, B., Bajaj-Elliott, M., MacDonald, T. T., Inglin, R., Eysselein, V. E., and Büchler, M. W. (2000) Characterisation of acute murine dextran sodium sulphate colitis. Cytokine profile and dose dependency. *Digestion* **62,** 240–248
4. Obermeier, F., Kojouharoff, G., Hans, W., Schölmerich, J., Gross, V., and Falk, W. (1999) Interferon-γ (IFN-γ)- and tumour necrosis factor (TNF)-induced nitric oxide as toxic effector molecule in chronic dextran sulphate sodium (DSS)-induced colitis in mice. *Clin. Exp. Immunol.* **116,** 238–245
5. Ito, R., Shin-Ya, M., Kishida, T., Urano, A., Takada, R., Sakagami, J., Imanishi, J., Kita, M., Ueda, Y., Iwakura, Y., Kataoka, K., Okanoue, T., and Mazda, O. (2006) Interferon-γ is causatively involved in experimental inflammatory bowel disease in mice. *Clin. Exp. Immunol.* **146,** 330–338
6. Collett, A., Higgs, N. B., Gironella, M., Zeef, L. A., Hayes, A., Salmo, E., Haboubi, N., Iovanna, J. L., Carlson, G. L., and Warhurst, G. (2008) Early molecular and functional changes in colonic epithelium that precede increased gut permeability during colitis development in mdr1a(−/−) mice. *Inflamm. Bowel Dis.* **14,** 620–631
7. Masunaga, Y., Noto, T., Suzuki, K., Takahashi, K., Shimizu, Y., and Morokata, T. (2007) Expression profiles of cytokines and chemokines in murine MDR1a−/− colitis. *Inflamm. Res.* **56,** 439–446
8. Staley, E. M., Schoeb, T. R., and Lorenz, R. G. (2009) Differential susceptibility of P-glycoprotein deficient mice to colitis induction by environmental insults. *Inflamm. Bowel Dis.* **15,** 684–696
9. Bruewer, M., Samarin, S., and Nusrat, A. (2006) Inflammatory bowel disease and the apical junctional complex. *Ann. N.Y. Acad. Sci.* **1072,** 242–252
10. Wang, F., Schwarz, B. T., Graham, W. V., Wang, Y., Su, L., Clayburgh, D. R., Abraham, C., and Turner, J. R. (2006) IFN-γ-induced TNFR2 expression is required for TNF-dependent intestinal epithelial barrier dysfunction. *Gastroenterology* **131,** 1153–1163
11. Silva, M. A. (2009) Intestinal dendritic cells and epithelial barrier dysfunction in Crohn's disease. *Inflamm. Bowel Dis.* **15,** 436–453
12. Bertelsen, L. S., Barrett, K. E., and Keely, S. J. (2004) G_s protein-coupled receptor agonists induce transactivation of the epidermal growth factor receptor in T_{84} cells. Implications for epithelial secretory responses. *J. Biol. Chem.* **279,** 6271–6279
13. Thongon, N., Nakkrasae, L. I., Thongbunchoo, J., Krishnamra, N., and Charoenphandhu, N. (2009) Enhancement of calcium transport in Caco-2 monolayer through PKCζ-dependent Cav1.3-mediated transcellular and rectifying paracellular pathways by prolactin. *Am. J. Physiol. Cell Physiol.* **296,** C1373–C1382
14. Uribe, J. M., Gelbmann, C. M., Traynor-Kaplan, A. E., and Barrett, K. E. (1996) Epidermal growth factor inhibits Ca^{2+}-dependent Cl^- transport in T84 human colonic epithelial cells. *Am. J. Physiol.* **271,** C914–C922
15. Keely, S. J., Uribe, J. M., and Barrett, K. E. (1998) Carbachol stimulates transactivation of epidermal growth factor receptor and mitogen-activated protein kinase in T_{84} cells. Implications for carbachol-stimulated chloride secretion. *J. Biol. Chem.* **273,** 27111–27117
16. Egger, B., Büchler, M. W., Lakshmanan, J., Moore, P., and Eysselein, V. E. (2000) Mice harboring a defective epidermal growth factor receptor (waved-2) have an increased susceptibility to acute dextran sulfate-induced colitis. *Scand. J. Gastroenterol.* **35,** 1181–1187
17. Egger, B., Procaccino, F., Lakshmanan, J., Reinshagen, M., Hoffmann, P., Patel, A., Reuben, W., Gnanakkan, S., Liu, L., Barajas, L., and Eysselein, V. E. (1997) Mice lacking transforming growth factor alpha have an increased susceptibility to dextran sulfate-induced colitis. *Gastroenterology* **113,** 825–832
18. Egger, B., Carey, H. V., Procaccino, F., Chai, N. N., Sandgren, E. P., Lakshmanan, J., Buslon, V. S., French, S. W., Büchler, M. W., and Eysselein, V. E. (1998) Reduced susceptibility of mice overexpressing transforming growth factor α to dextran sodium sulphate induced colitis. *Gut* **43,** 64–70
19. McCole, D. F., Rogler, G., Varki, N., and Barrett, K. E. (2005) Epidermal growth factor partially restores colonic ion transport responses in mouse models of chronic colitis. *Gastroenterology* **129,** 591–608
20. Sinha, A., Nightingale, J., West, K. P., Berlanga-Acosta, J., and Playford, R. J. (2003) Epidermal growth factor enemas with oral mesalamine for mild-to-moderate left-sided ulcerative colitis or proctitis. *New Engl. J. Med.* **349,** 350–357
21. Weymer, A., Huott, P., Liu, W., McRoberts, J. A., and Dharmsathaphorn, K. (1985) Chloride secretory mechanism induced by prostaglandin E_1 in a colonic epithelial cell line. *J. Clin. Invest.* **76,** 1828–1836
22. Augeron, C., and Laboisse, C. L. (1984) Emergence of permanently differentiated cell clones in a human colonic cancer cell line in culture after treatment with sodium butyrate. *Cancer Res.* **44,** 3961–3969
23. Uribe, J. M., McCole, D. F., and Barrett, K. E. (2002) Interferon-γ activates EGF receptor and increases TGF-α in T84 cells. Implications for chloride secretion. *Am. J. Physiol. Gastrointest. Liver Physiol.* **283,** G923–G931
24. Okayasu, I., Hatakeyama, S., Yamada, M., Ohkusa, T., Inagaki, Y., and Nakaya, R. (1990) A novel method in the induction of reliable experimental acute and chronic ulcerative colitis in mice. *Gastroenterology* **98,** 694–702

25. Burova, E., Vassilenko, K., Dorosh, V., Gonchar, I., and Nikolsky, N. (2007) Interferon gamma-dependent transactivation of epidermal growth factor receptor. *Fed. Eur. Biochem. Soc. Lett.* **581,** 1475–1480
26. Scharl, M., Paul, G., Barrett, K.E., and McCole, D. F. (2009) AMP-activated protein kinase mediates the interferon-γ-induced decrease in intestinal epithelial barrier function. *J. Biol. Chem.* **284,** 27952–27963
27. Chow, J. Y., Uribe, J. M., and Barrett, K. E. (2000) A role for protein kinase Cε in the inhibitory effect of epidermal growth factor on calcium-stimulated chloride secretion in human colonic epithelial cells. *J. Biol. Chem.* **275,** 21169–21176
28. Flores, C. A., Melvin, J. E., Figueroa, C. D., and Sepúlveda, F. V. (2007) Abolition of Ca^{2+}-mediated intestinal anion secretion and increased stool dehydration in mice lacking the intermediate conductance Ca^{2+}-dependent K^+ channel Kcnn4. *J. Physiol.* **583,** 705–717
29. Halm, S. T., Liao, T., and Halm, D. R. (2006) Distinct K^+ conductive pathways are required for Cl^- and K^+ secretion across distal colonic epithelium. *Am. J. Physiol. Cell Physiol.* **291,** C636–C648
30. Schultheiss, G., and Diener, M. (1997) Regulation of apical and basolateral K^+ conductances in rat colon. *Br. J. Pharmacol.* **122,** 87–94
31. DuVall, M. D., Guo, Y., and Matalon, S. (1998) Hydrogen peroxide inhibits cAMP-induced Cl^- secretion across colonic epithelial cells. *Am. J. Physiol.* **275,** C1313–C1322
32. Wang, D., Yang, E. B., Lek, L. H., and Cheng, L. Y. (1997) Transmodulation of EGF receptor by interferon-γ in human hepatocellular carcinoma HepG2 cells. *In Vivo* **11,** 141–146
33. Hamburger, A. W., and Pinnamaneni, G. D. (1991) Increased epidermal growth factor receptor gene expression by γ-interferon in a human breast carcinoma cell line. *Br. J. Cancer* **64,** 64–68
34. Johnson, H. M., Subramaniam, P. S., Olsnes, S., and Jans, D. A. (2004) Trafficking and signaling pathways of nuclear localizing protein ligands and their receptors. *BioEssays* **26,** 993–1004
35. Hassan, S. W., Doody, K. M., Hardy, S., Uetani, N., Cournoyer, D., and Tremblay, M. L. (2010) Increased susceptibility to dextran sulfate sodium induced colitis in the T cell protein tyrosine phosphatase heterozygous mouse. *PLOS One* **5,** e8868
36. Heinonen, K. M., Bourdeau, A., Doody, K. M., and Tremblay, M. L. (2009) Protein tyrosine phosphatases PTP-1B and TC-PTP play nonredundant roles in macrophage development and IFN-γ signaling. *Proc. Natl. Acad. Sci. U.S.A.* **106,** 9368–9372
37. McCole, D. F., Truong, A., Bunz, M., and Barrett, K. E. (2007) Consequences of direct versus indirect activation of epidermal growth factor receptor in intestinal epithelial cells are dictated by protein-tyrosine phosphatase 1B. *J. Biol. Chem.* **282,** 13303–13315
38. Scharl, M., Paul, G., Weber, A., Jung, B. C., Docherty, M. J., Hausmann, M., Rogler, G., Barrett, K. E., and McCole, D. F. (2009) Protection of epithelial barrier function by the Crohn's disease associated gene protein tyrosine phosphatase n2. *Gastroenterology* **137,** 2030–2040.e5
39. Tonks, N. K. (2003) PTP1B: from the sidelines to the front lines. *Fed. Eur. Biochem. Soc. Lett.* **546,** 140–148
40. DeYulia, G. J., Jr., and Cárcamo, J. M. (2005) EGF receptor-ligand interaction generates extracellular hydrogen peroxide that inhibits EGFR-associated protein tyrosine phosphatases. *Biochem. Biophys. Res. Commun.* **334,** 38–42
41. McCole, D. F., Keely, S. J., Coffey, R. J., and Barrett, K. E. (2002) Transactivation of the epidermal growth factor receptor in colonic epithelial cells by carbachol requires extracellular release of transforming growth factor-α. *J. Biol. Chem.* **277,** 42603–42612
42. Barrett, K. E., Smitham, J., Traynor-Kaplan, A., and Uribe, J. M. (1998) Inhibition of Ca^{2+}-dependent Cl- secretion in T84 cells. Membrane target(s) of inhibition is agonist specific. *Am. J. Physiol.* **274,** C958–C965
43. Trzcinski, R., Bry, M., Krajewska, W., Kulig, M., and Dzyiki, A. (2004) ErbB-1 expression in experimental model of inflammatory bowel disease in rats. *Acta Chir. Iugosl.* **51,** 85–89
44. Sottili, M., Sternini, C., Reinshagen, M., Brecha, N. C., Nast, C. C., Walsh, J. H., and Eysselein, V. E. (1995) Up-regulation of transforming growth factor α binding sites in experimental rabbit colitis. *Gastroenterology* **109,** 24–31
45. Egan, L. J., de Lecea, A., Lehrman, E. D., Myhre, G. M., Eckmann, L., and Kagnoff, M. F. (2003) Nuclear factor-κB activation promotes restitution of wounded intestinal epithelial monolayers. *Am. J. Physiol. Cell Physiol.* **285,** C1028–C1035
46. Myhre, G. M., Toruner, M., Abraham, S., and Egan, L. J. (2004) Metalloprotease disintegrin-mediated ectodomain shedding of EGFR ligands promotes intestinal epithelial restitution. *Am. J. Physiol. Gastrointest. Liver Physiol.* **287,** G1213–G1219
47. Hoffmann, P., Reinshagen, M., Zeeh, J. M., Lakshmanan, J., Wu, V. S., Goebell, H., Gerken, G., and Eysselein, V. E. (2000) Increased expression of epidermal growth factor-receptor in an experimental model of colitis in rats. *Scand. J. Gastroenterol.* **35,** 1174–1180
48. Procaccino, F., Reinshagen, M., Hoffmann, P., Zeeh, J. M., Lakshmanan, J., McRoberts, J. A., Patel, A., French, S., and Eysselein, V. E. (1994) Protective effect of epidermal growth factor in an experimental model of colitis in rats. *Gastroenterology* **107,** 12–17
49. Frey, M. R., Edelblum, K. L., Mullane, M. T., Liang, D., and Polk, D. B. (2009) The ErbB4 growth factor receptor is required for colon epithelial cell survival in the presence of TNF. *Gastroenterology* **136,** 217–226
50. Colgan, S. P., Parkos, C. A., Matthews, J. B., D'Andrea, L., Awtrey, C. S., Lichtman, A. H., Delp-Archer, C., and Madara, J. L. (1994) Interferon-γ induces a cell surface phenotype switch on T84 intestinal epithelial cells. *Am. J. Physiol.* **267,** C402–C410
51. Galietta, L. J., Folli, C., Marchetti, C., Romano, L., Carpani, D., Conese, M., and Zegarra-Moran, O. (2000) Modification of transepithelial ion transport in human cultured bronchial epithelial cells by interferon-γ. *Am. J. Physiol. Lung Cell Mol. Physiol.* **278,** L1186–L1194
52. Sugi, K., Musch, M. W., Field, M., and Chang, E. B. (2001) Inhibition of Na^+,K^+-ATPase by interferon γ down-regulates intestinal epithelial transport and barrier function. *Gastroenterology* **120,** 1393–1403
53. Devor, D. C., Singh, A. K., Bridges, R. J., and Frizzell, R. A. (1997) Psoralens. Novel modulators of Cl^- secretion. *Am. J. Physiol.* **272,** C976–C988
54. Keely, S. J., and Barrett, K. E. (1999) ErbB2 and ErbB3 receptors mediate inhibition of calcium-dependent chloride secretion in colonic epithelial cells. *J. Biol. Chem.* **274,** 33449–33454
55. Keely, S. J., Calandrella, S. O., and Barrett, K. E. (2000) Carbachol-stimulated transactivation of epidermal growth factor receptor and mitogen-activated protein kinase in T_{84} cells is mediated by intracellular Ca^{2+}, PYK-2, and $p60^{src}$. *J. Biol. Chem.* **275,** 12619–12625
56. Heitzmann, D., and Warth, R. (2008) Physiology and pathophysiology of potassium channels in gastrointestinal epithelia. *Physiol. Rev.* **88,** 1119–1182
57. Nielsen, M. S., Warth, R., Bleich, M., Weyand, B., and Greger, R. (1998) The basolateral Ca^{2+}-dependent K^+ channel in rat colonic crypt cells. *Pflugers Archiv.* **435,** 267–272
58. Hoque, K. M., Rajendran, V. M., and Binder, H. J. (2005) Zinc inhibits cAMP-stimulated Cl secretion via basolateral K-channel blockade in rat ileum. *Am. J. Physiol. Gastrointest. Liver Physiol.* **288,** G956–G963